A flexure-based gripper for small-scale manipulation

Michael Goldfarb and Nikola Celanovic

Department of Mechanical Engineering, Vanderbilt University, Box 1592, Station B, Nashville TN 37235 (USA)

(Received in Final Form: June 12, 1998)

SUMMARY
A small-scale flexure-based gripper was designed for manipulation tasks requiring precision position and force control. The gripper is actuated by a piezoelectric ceramic stack actuator and utilizes strain gages to measure both the gripping force and displacement. The position and force bandwidths were designed for ten Hertz and one hundred Hertz, respectively, in order to afford human-based teleoperative transparency. The gripper serves effectively as a one degree-of-freedom investigation of compliant mechanism design for position and force controlled micromanipulation. Data is presented that characterizes the microgripper performance under both pure position and pure force control, followed by a discussion of the attributes and limitations of flexure-based design.

KEYWORDS: Microgripper; Micromanipulation; Flexure-based design; Control.

1. INTRODUCTION
Though considerable research has been directed toward the advancement of robotic manipulation on a conventional scale (i.e. millimeters to meters), relatively little work has been conducted on interactive robotic manipulation at a microscopic scale (i.e., microns to millimeters). Once developed, interactive micromanipulator technology will have application in many fields, including micromanufacturing, microsurgery, telesurgery, microbiology and pharmaceutical research. Many microscale parts, for example, have been fabricated utilizing photo lithographic and X-ray lithographic microfabrication techniques. Despite these advanced microfabrication techniques, fully functional multielement microelectromechanical (MEMS) devices have not yet come to fruition, due in part to the inability to assemble the very small parts, and in particular to assemble in large quantities (i.e., mass produce). A micromanipulator would enable dexterous handling of micromanufactured parts, and thus enable assembly of functional MEMS devices. If utilized in a teleoperative sense, a macromanipulator master coupled to a micromanipulator slave could enable dexterous human-controlled telemanipulation of a microscopic environment. In this sense, the telemanipulation system would address human positioning limitations in the forward path and limited human force sensitivity in the backward path. Coupled with a stereomicroscope, this technology would enable dexterous interaction between a human and a microscopic environment.

Operation in small-scale, often delicate environments requires stable and precise control of manipulator motion and force. Interactive manipulation, in particular, often requires simultaneous control of both position and force, and in general, in a non-orthogonal manner. Several methodologies have been proposed for dynamically interactive control, including impedance,[1] stiffness,[2] and hybrid position/force control.[3,4] One of the most significant impediments to effective implementation of such control is the presence of hard nonlinearities, in particular backlash and Coulomb friction, in the open loop manipulator mechanics.[5–9] The study of direct-drive robots was borne out of the necessity to implement precision position and force control of robot manipulation for purposes of mechanical interaction.[10] A direct-drive design significantly reduces the amount of backlash and Coulomb friction in the control plant. The elimination of these hard nonlinearities facilitates effective and accurate position, force, impedance, or admittance control of a robot manipulator.

Due to the physics of scaling, devices that operate on a microscopic scale are influenced by highly nonlinear surface forces to a much greater degree than those of a conventional scale.[11,12] Conventional-scale manipulator behavior is typically dominated by inertial effects, which are fundamentally smooth and tend to filter the effects of hard nonlinearities on manipulator motion. The significance of inertial mechanics, however, diminishes with decreasing scale. The magnitude of inertial forces is typically in proportion to volume (assuming invariance of density), and thus scales with the cube of the geometric scaling ratio. As friction is a surface force, the magnitude scales conservatively in proportion to surface area, and thus scales with the square of the geometric scaling ratio. Geometrically similar but smaller devices therefore exhibit increased surface effects and decreased inertial effects, thus exacerbating the control problems presented by non-smooth nonlinearities. If Coulomb friction is independent of surface area, as the conventional conception suggests, then the increased ratio of friction to inertial effects at decreasing scales is even greater.

2. COMPLIANT MECHANISM DESIGN
The adverse effects of hard nonlinearities on the performance of robot manipulation (and especially micromanipulation) can be avoided by designing compliant mechanism-based "smooth" manipulators. A compliant mechanism is a device that moves solely by deformation, typically by utilizing flexures in place of conventional bearings. Since these devices do not entail any sliding or

rolling, they are free of backlash and Coulomb friction, and thus have perfectly smooth mechanics. In addition to significantly enhancing control stability, the absence of hard nonlinearities in compliant mechanism behavior places no fundamental physical limitations on the resolution of position or force control. Additionally, the absence of conventional joints and bearing surfaces produces a clean device that is free of lubricants or other contaminants, and thus is extremely conducive to clean environments. The gripper design described in this paper is essentially a one degree-of-freedom investigation of a flexure-based position and force-controlled microrobot design.

3. MICROGRIPPER DESIGN

Since the microgripper was designed for use in a human-controlled teleoperative system, many of the design specifications were derived from human capability. The human motor control system exhibits position and force bandwidths on the order of ten and one hundred Hertz, respectively.[13] A transparent telemanipulation system therefore requires an actuator that exhibits comparable bandwidths and sufficient power to perform work in the environment of interest. Additionally, control stability is best served with open-loop stable actuators that, like the compliant mechanism, exhibit smooth behavior. The range of motion and gripping force required of a microgripper is largely dependent upon application. The microgripper described in this paper was designed to offer a gripping workspace approximately two orders of magnitude smaller than the typical human prehensile grip. Such scaling requires a range of motion of 500 microns and suggests an appropriate gripping force of 500 mN.

Prior work by the authors indicate that piezoelectric ceramic, coupled with an appropriate transmission (devoid of bearing surfaces), can provide the desired actuation performance.[14,15] A typical lead-zirconate-titanate (PZT) piezoelectric stack actuator can perform step movements with a resolution on the order of a nanometer. These

actuators offer open-loop stable operation with the power and bandwidth necessary for the specified motion. The primary inadequacy of the PZT as a microrobotic actuator is that the strain-based deformations that it provides are limited to approximately 0.1%. A piezoelectric stack that could provide the desired displacement of 500 microns in a direct-drive fashion would therefore have to be one half meter in length. Since piezoelectric ceramic actuators operate in compression, stack geometry is typically constrained by buckling considerations to significantly shorter lengths. The piezoelectric stack incorporated for actuation
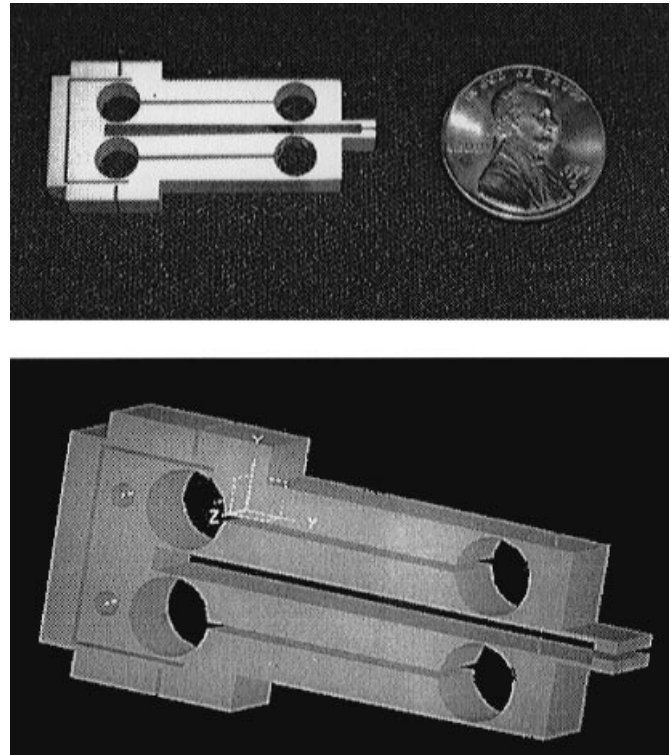

Fig. 1. (top) Flexure-based microgripper structure and transmission and (bottom) solid model of gripper design.
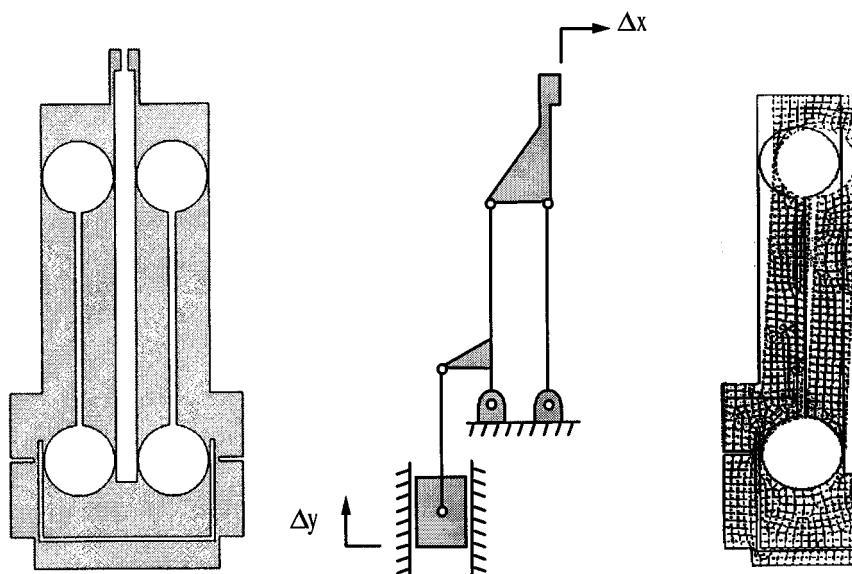

Fig. 2. (left) Two-dimensional drawing of microgripper structure, (middle) idealized schematic of (one half of) flexure-based linkage, and (right) finite element analysis illustrating motion of (one half of) gripper.
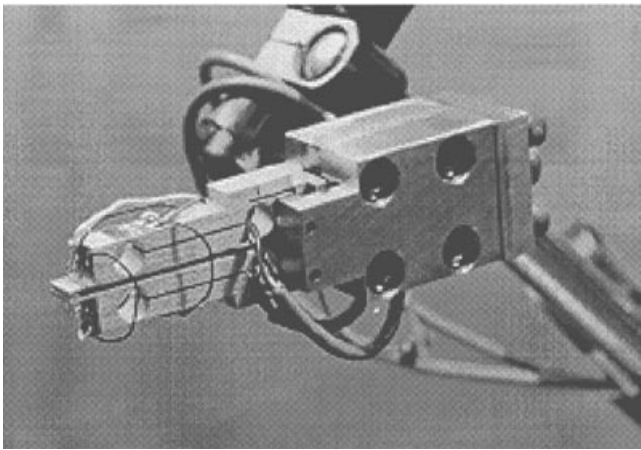
Fig. 3. Instrumented microgripper prototype.

of the flexure-based microgripper is twenty millimeters in length (Tokin model #AE0505D16) and is therefore capable of approximately twenty microns of no load displacement. Incorporating a piezoelectric stack for actuation of the microgripper therefore requires a large ratio transmission that is devoid of Coulomb friction and backlash. This transmission in the gripper is provided by the compliant mechanism shown in Figure 1. The mechanism approximates the linkage illustrated in Figure 2, and provides a transmission ratio of about thirty-to-one and parallel closure of the gripping tongs. The transmission affords a total gripping motion and a maximum gripping force of approximately 500 microns and one Newton, respectively, from the PZT actuator. The gripper prototype is 36 mm long, 16.5 mm wide, and 5 mm thick. The gripper was fabricated from a single piece of 7075 aluminium alloy with a wire electrical discharge machine process.

The flexure-based structure of the gripper was additionally designed to decouple strains due to gripper position and force. This design enables the use of strain gages for independent measurement of gripper position and force. The microgripper prototype, complete with sensors and PZT actuator (housed), is shown in Figure 3.

4. MICROGRIPPER PERFORMANCE
Position control of the microgripper tongs was achieved utilizing a digitally implemented proportional-integral-derivative (PID) controller with a feed-forward term, as illustrated in Figure 4. The feed-forward term represents a
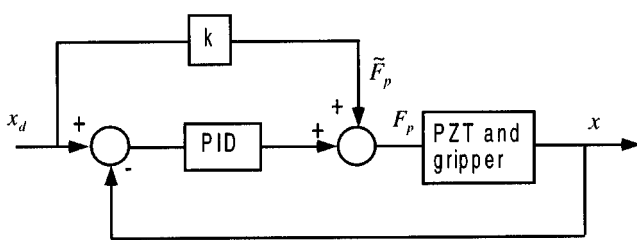

Fig. 4. PZT-actuated compliant mechanism position controller. The feed-forward term is a simple quasi-static model of the PZT and compliant mechanism (i.e., a pure stiffness), which provides a command estimate for the desired position, and the PID loop provides correction of the estimate for model error.

simple quasi-static model of the PZT and compliant mechanism (i.e. a pure stiffness), which provides a command estimate for the desired position, and the PID loop provides correction of the estimate for model error. The position control loop frequency response is shown in Figure 5. As indicated in the figure, the position control frequency response begins to roll off (-3 dB) around 40 Hertz. Closed-loop time domain behavior is illustrated by the tracking data shown in Figure 6. Not that the rising and falling step responses of the square wave tracking in Figure 6 are slightly different. Since piezoelectric actuators operate in a compressive mode (i.e. they cannot provide tensile actuation forces), the return forces are provided by the elastic behavior of a compliant mechanism. This arrangement renders one direction of motion a forced response and the other a characteristic response of the structure. Such a configuration entails a trade-off between a high positional bandwidth, which is dependent on a large joint stiffness, and a large output force, which is dependent on a low stiffness.
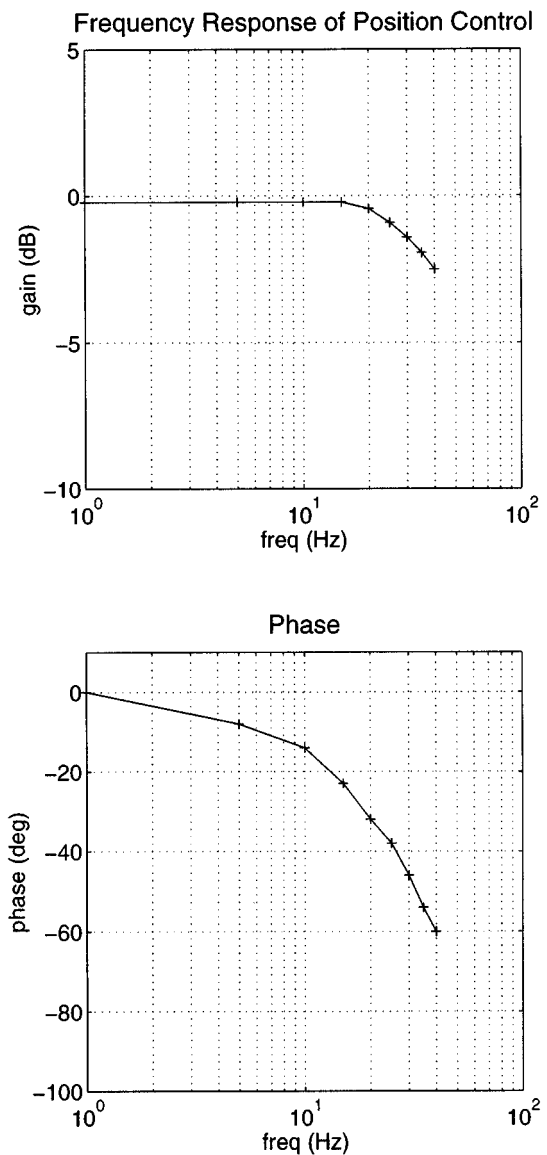
Force control of the microgripper tongs was also

Fig. 5. Frequency response of position control loop. Data was acquired at a 5 kHz controller sampling rate.
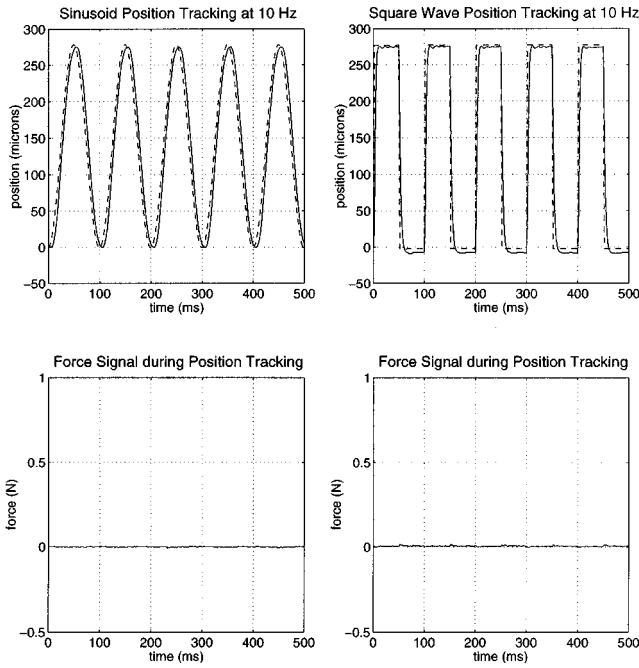
Fig. 6. Closed-loop time domain behavior of position control loop for a 10 Hz sinusoid (left column) and square wave (right column), showing the desired (dashed) and the actual (solid) position, and the corresponding force sensor signals (illustrating sensor decoupling).

implemented utilizing a digitally implemented proportional-integral-derivative (PID) controller with a feed-forward term, as illustrated in Figure 7. The added complexity of the feed-forward term in the force controller is due to reconstruction of gripper position. The feedback loop in the feed-forward term could be eliminated if gripper position were measured rather than estimated. As with the position controller, the feed-forward term provides a model-based estimate of the control effort, and the PID loop provides correction of this estimate. The force control loop frequency response is shown in Figure 8, which as shown rolls off above 100 Hz. The roll-off exhibited by the system reflects limitations imposed by computational delays of the digitally implemented controller, which is the slowest element of the
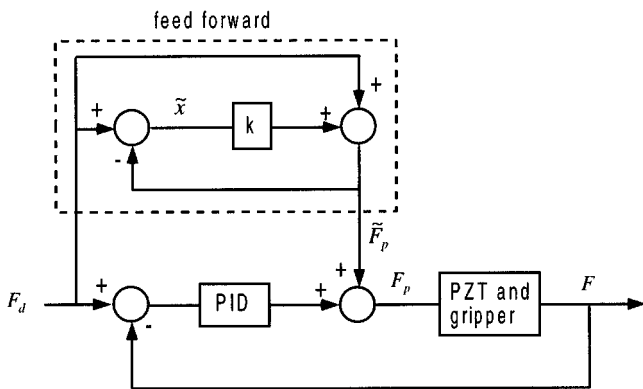

Fig. 7. PZT-actuated compliant mechanism force controller. The feed-forward term is a simple quasi-static model of the PZT and compliant mechanism (i.e., a pure stiffness) that includes a state estimator for estimating position. The feed-forward model provides a command estimate for the desired position, and the PID loop provides correction of the estimate for model error.

force control system. Closed-loop time domain behavior is illustrated by the tracking data shown in Figure 9.

5. DISCUSSION OF FLEXURE-BASED DESIGN

1. Flexure-Based versus Conventional Mechanisms

A flexure-based joint is devoid of Coulomb friction and backlash, but entails several disadvantages relative to a conventional revolute joint. The primary problems with flexure joints are the limited range of angular motion, the stiffness exhibited along the direction of rotation, and the compliance exhibited in directions orthogonal to the direction of rotation. The angular range of motion of a flexure joint is limited by the elastic range of material deformation in the joint, which is influenced by the geometry and the material properties of the joint. A joint of typical metal alloy and geometry, such as that shown in Figure 10 (top), is limited to angular displacements on the order of a few degrees. A greater range of motion can be
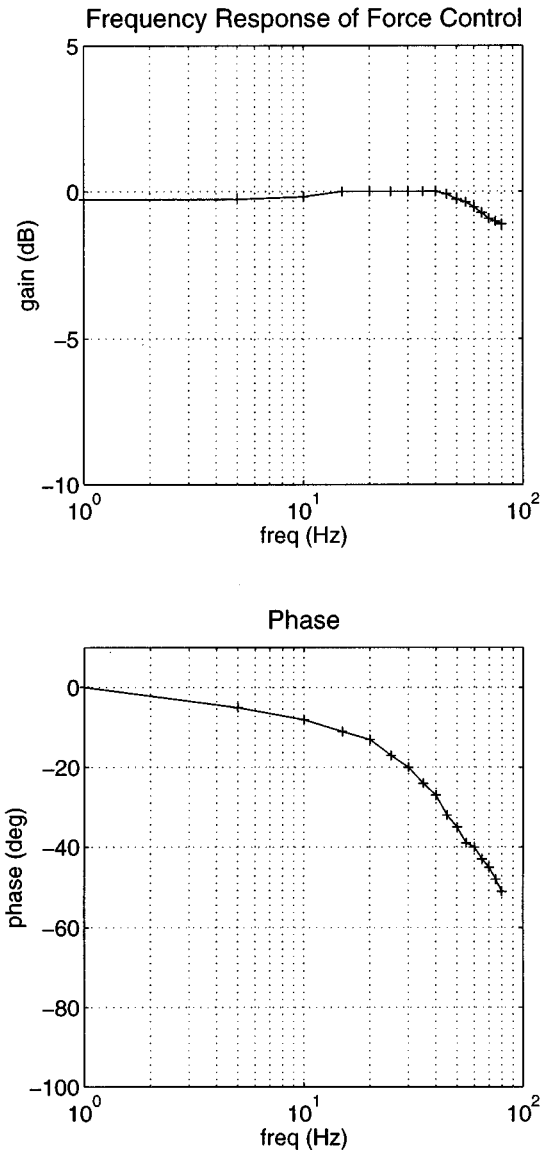

Fig. 8. Frequency response of force control loop. Data was acquired at a 5 kHz controller sampling rate.

achieved by utilizing plastic deformation, but such an approach results in rapid fatigue failure. In fact, given the stress concentration imposed by a flexure joint, avoiding high cycle fatigue typically requires the stresses in the joint be limited to approximately one fourth of the material elastic limit. Horie et al. have recently developed super-elastic flexure hinges that incorporate shape memory alloy in a thin, flat geometry that provide angular displacements up to thirty degrees.[16] Such geometry, however, which is depicted in Figure 10 (middle), trades increased range of motion for compliance exhibited in directions orthogonal to the direction of rotation, which is another significant problem with flexure joints. Specifically, an ideal revolute joint has no stiffness along the direction of rotation and is infinitely stiff in all other directions. In contrast, a flexure joint exhibits stiffness along the direction of rotation and compliance in all other directions. This notion is illustrated by the diagram shown in Figure 10 (bottom). In the figure, the stiffness in the direction of rotation is given by M_x/ϕ_x, while the stiffnesses that are orthogonal to the direction of rotation are those given by M_y/ϕ_y, M_z/ϕ_z, F_x/x, and F_y/y. In general, the geometric properties that enable an increased range of motion and decreased stiffness along the direction of rotation also result in compliance along axes orthogonal

to the rotational axis. The thin, flat super-elastic hinge of Horie et al., for example, is considerably more susceptible to tension/compression compliance, torsional compliance and compressive buckling than a more compact geometry. Such behavior is particularly significant in multi-degree-of-freedom manipulators that operate in high impedance environments.

2. Attainable Output in PZT-Actuated Compliant Mechanisms

Figure 11 (top) shows a simple quasi-static model of a PZT stack actuator, where x_p is the actuator displacement, k_p is the elastic stiffness of the ceramic, F_p is an internal force which is proportional to the applied voltage, and F_o is the external actuation force (see references[14–15] for a more accurate dynamic model). Figure 11 (bottom) depicts the region of operation (i.e. the attainable output) of the actuator. A conventional mechanism may distort this region to provide more or less force or displacement, but will essentially preserve the area of the region. A compliant mechanism, however, will decrease the area, and thus reduce the effectiveness of the mechanism. The two primary sources of energy storage in a compliant mechanism are the rotational joint compliance (energy storage along the
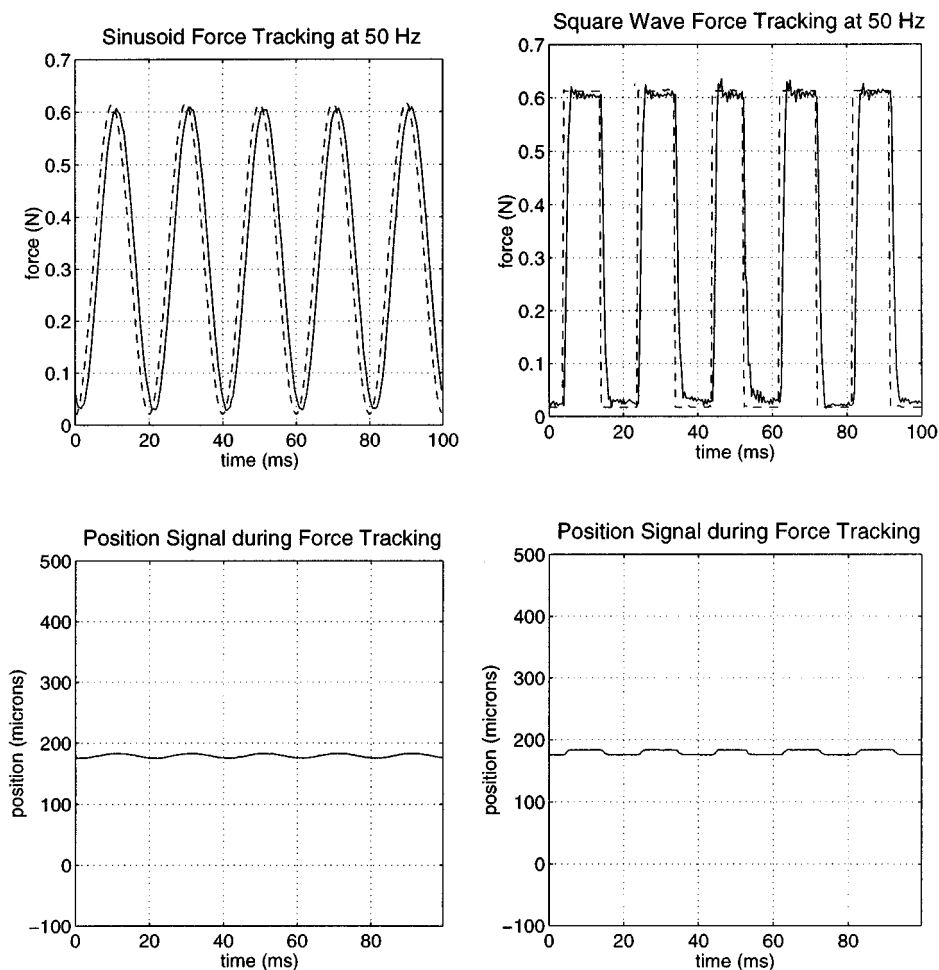

Fig. 9. Closed-loop time domain behavior of force control loop for a 50 Hz sinusoid (left column) and square wave (right column), showing the desired (dashed) and the actual (solid force), and the corresponding position sensor signals (illustrating sensor decoupling). Note that the fluctuations in the position signal are due to compliance of the object and limited stiffness of the gripper structure, rather than fundamental sensor coupling.
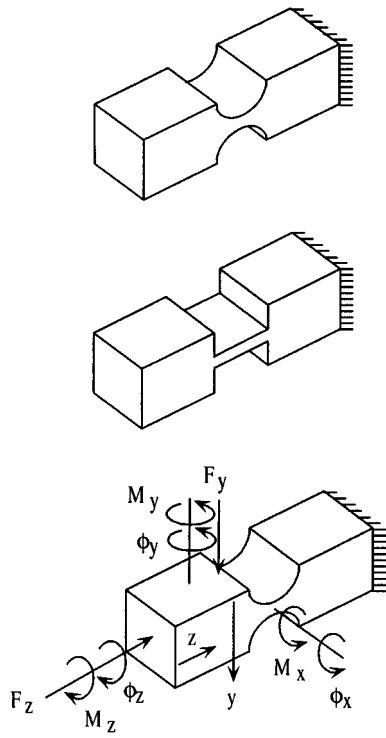
Fig. 10. (top) Typical flexure geometry, (middle) thin, flat flexure geometry, such as the super-elastic flexure of Horie et al., and (bottom) loading diagram illustrating the stiffness along the direction of rotation and compliance in all other directions.

desired kinematic trajectory of the mechanism) and the link compliance (energy storage orthogonal to the desired kinematic trajectory), each of which affect the region of operation in a different manner. Figure 12 (top) depicts a model of a PZT actuator driving a compliant mechanism with compliant joints and rigid links. In this case, the rotational joint stiffness k_j acts in parallel to the stiffness of the actuator (i.e. along the kinematic trajectory of the
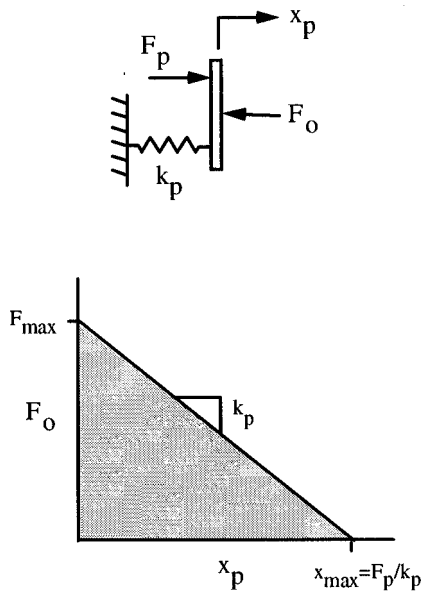

Fig. 11. (top) Quasi-static model of PZT stack actuator and (bottom) region of attainable output (region of operation).
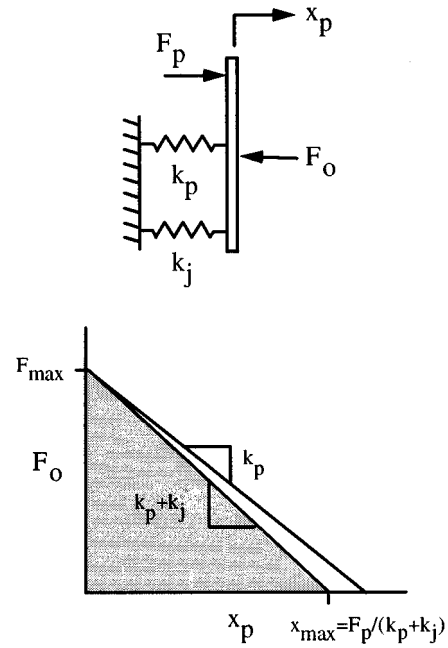

Fig. 12. (top) Quasi-static model of PZT with compliant mechanism joint stiffness and (bottom) region of attainable output (region of operation).

mechanism), so the slope of the line that defines the region of operation is $k_p + k_j$. The change in slope effectively limits the maximum no-load output displacement, but does not affect the blocked output force, as illustrated in Figure 12 (bottom). Conventional mechanisms are often assumed to have rigid links. This assumption, however, is typically not accurate when utilizing a PZT-actuated compliant mechanism in a high impedance environment. Structural deformation in a loaded compliant mechanism derives from compressive, tensile, and shear deformation of the flexure joints, in addition to structural deformation of the mechanism links. These combined effects can be lumped into a single structural stiffness k_s, which acts in series with the actuator (i.e. orthogonal to the kinematic trajectory of the mechanism), as illustrated in Figure 13 (top). The resulting region of operation, which is shown in Figure 13 (bottom), is defined by a line of slope $(k_p + k_j)k_s/(k_p + k_j + k_s)$. The change in slope effectively limits the maximum blocked force, but does not affect the no-load output displacement of the mechanism.

3. Implications for Optimal Design

The net effect of the joint rotational stiffness is to limit the range of output motion. One might therefore assume that optimal joint geometry would produce a minimum rotational stiffness k_j. This is typically the case when the mechanism is designed to operate in a low impedance environment (i.e. little or no output force). When operating in a high impedance environment (i.e. exerting significant output force), however, joint geometry that results in low rotational stiffness is typically sub-optimal. This is because the geometric and material properties that enable a low rotational stiffness also tend to decrease the compliance in other directions. Structural deformation orthogonal to the
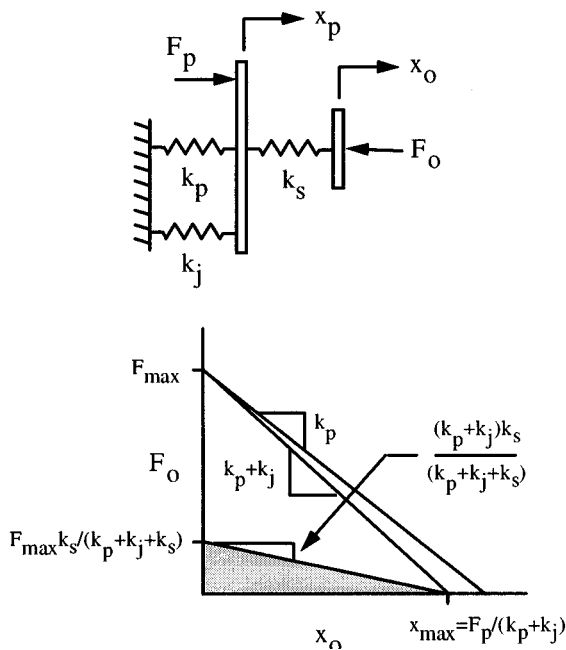
Fig. 13. (top) Quasi-static model of PZT with compliant mechanism joint stiffness and structural compliance and (bottom) region of attainable output (region of operation).

desired kinematic trajectory does not significantly affect the behavior of the mechanism in a low impedance environment because, in such an environment, the device will operate in the region near the horizontal (displacement) axis of Figure 13 (bottom). In a high impedance environment, however, the device will generally operate along the vertical (force) axis, where the effects of non-kinematic structural elasticity are particularly noticeable. Optimal flexure joint design will therefore entail a trade-off between maximum no-load displacement (minimizing k_j) and maximum blocked force output (maximizing k_s). Additionally, optimal joint geometry will in general be different for each joint in the mechanism, depending upon the joint angular rotation, the tensile or compressive loading, the kinematic sensitivity of the mechanism to joint deformation, and the nature of the environment. Optimal flexure joint geometry is therefore best derived with an analytical model-based design optimization of the mechanism. Such an optimization is aided by analytical expressions for the stiffness of typical flexure joint geometries, which can be found in the references.[17–18]

6. CONCLUSION

A flexure-based microgripper was developed and shown to exhibit well-behaved stable position and force control utilizing relatively simple controllers. The compliant mechanism design approach therefore seems well suited for precision micromanipulator applications that entail mechanical interaction, such as a telemicrorobot. The smooth behavior of the flexure-based design, however, is achieved at the cost of limited joint motion and a reduction of the attainable force/displacement output of the actuator.

References
1. N. Hogan, "Impedance control: an approach to manipulation" *ASME Journal of Dynamic Systems, Measurement, and Control* **107**, 1–24 (1985).
2. J.K. Salisbury, "Active stiffness control of a manipulator in cartesian coordinates" *Proceedings of the IEEE Conference on Decision and Control* (1980) pp. 95–100.
3. M. Raibert and J. Craig, "Hybrid position/force control of manipulators" *ASME Journal of Dynamic Systems, Measurement, and Control* **103**, 126–133 (1981).
4. T. Yoshikawa, "Hybrid control theory of robot manipulators" *Proceedings of the Sixth International Symposium for Robotics Research* (1993) pp. 443–452.
5. N.G. Chalhoub and A.G. Ulsoy, "Effect of a self-locking drive mechanism on the performance of a flexible robot arm" *Proceedings of the American Control Conference* (1990) pp. 1270–1271.
6. Gogoussis and M. Donath, "Determining the effects of Coulomb friction on the dynamics of bearings and transmissions in robot mechanisms" *ASME Journal of Mechanical Design* **115**, No. 2, 231–240 (1993).
7. E.S. Nakagawa, Y. Uetake and Z. Cai, "Vibration analysis of robot manipulators: the effect of backlash in transmission mechanisms" *Transactions of the Japan Society of Mechanical Engineers* **57**, No. 544, 3877–3881 (1991).
8. H. Schempt and D.R. Yoerger, "Study of dominant performance characteristics in robot transmission" *ASME Journal of Mechanical Design* **115**, No. 3, 472–482 (1993).
9. W.T. Townsend and J.K. Salisbury, "The effect of Coulomb friction and stiction on force control" *Proceedings of the IEEE Conference on Robotics and Automation* (April 1987), pp. 883–889.
10. H. Asada and K. Youcef-Toumi, *Direct-Drive Robots: Theory and Practice* (MIT Press, Cambridge, Mass., 1987).
11. R. Fearing, "Survey of Sticking Effects for Micro Parts Handling" *Proceedings of the IEEE/RSJ Conference on Intelligent Robots and Systems* (1995) **Vol. 2**, pp. 212–217.
12. W. Trimmer and R. Jebens "Actuators for micro robots." *Proceedings of the IEEE International Conference on Robotics and Automation* (1989) pp. 1547–1552.
13. P. Fischer, R. Daniel and K.V. Siva, "Specification and design of input devices for teleoperation" *Proceedings of the IEEE Conference on Robotics and Automation* (May 1990) pp. 540–545.
14. M. Goldfarb and N. Celanovic, "A Lumped-Parameter Electromechanical Model for Describing the Nonlinear Behavior of Piezoelectric Actuators" *ASME Journal of Dynamic Systems, Measurement, and Control* **119**, No. 3, 478–485 (1997).
15. M. Goldfarb and N. Celanovic, "Modelling Piezoelectric Stack Actuators for Control of Micromanipulation" *IEEE Control Systems Magazine* **17**, No. 3, 69–79 (1997).
16. M. Horie, T. Nozaki, K. Ikegami, and F. Kobayashi, "Design system of super elastic hinges and its application to manipulator for micro-bonding by adhesives" *Proceedings of the International Symposium on Microsystems, Intelligent Materials, and Robots* (1995) pp. 185–188.
17. J. Paros and L. Weisbord, "How to design flexure hinges" *Machine Design* **37**, No. 27, 151–156 (1965).
18. K. Ragulskis, M. Arutunian, A. Kochikian and M. Pogosian, "A study of fillet type flexure hinges and their optimal design" *Vibration Engineering* **3**, 447–452 (1989).